The existence of multiple systems of stellar arcs implies that their progenitors originate in dense stellar clusters owing to stellar encounters and are ejected from them on subsequent approaches. Most likely, the progenitors of gamma-ray bursts escape from the cluster during the short and possibly repetitive stage of a maximum density of its core.

The specific mechanism of star formation induced by the jets of gamma-ray bursts is not understood. One can concede that the moving surface of the interaction between the jet and the ambient gas rakes the gas together, and the density of the resultant segment of the spherical surface eventually becomes high enough for star formation. Be it as it may, it is well known that active star formation is observed in a number of galaxies, being induced by relativistic jets emanating from the galactic nuclei.

References

1. Efremov Yu N *Pis'ma Astron. Zh.* **5** 21 (1979) [*Sov. Astron. Lett.* **5** 12 (1979)]
2. Efremov Yu N *Ochagi Zvezdoobrazovaniya v Galaktikakh* (Star Formation Centers in Galaxies) (Moscow: Nauka, 1989)
3. Efremov Yu N, Elmegreen B G *Mon. Not. R. Astron. Soc.* **299** 588 (1988)
4. Efremov Yu N *Astron. J.* **110** 2757 (1995)
5. Elmegreen B G, Efremov Yu N *Astrophys. J.* **466** 802 (1996)
6. Hayward R *Publ. ASP* **76** 35 (1964)
7. Westerlund B E, Mathewson D S *Mon. Not. R. Astron. Soc.* **131** 371 (1966)
8. Hodge P W *Publ. ASP* **79** 29 (1967)
9. Efremov Yu N, Elmegreen B G *Mon. Not. R. Astron. Soc.* **299** 643 (1998)
10. Braun J M, De Boer K S, Altmann M, astro-ph/0006060 (submitted to *Astron. Astrophys.*)
11. Postnov K A *Usp. Fiz. Nauk* **169** 545 (1999) [*Phys. Usp.* **42** 469 (1999)]
12. Blinnikov S I, Postnov K A *Mon. Not. R. Astron. Soc.* **293** L29 (1998)
13. Efremov Yu N, Elmegreen B G, Hodge P W *Astrophys. J.* **501** L163 (1998)
14. Spruit H C *Astron. Astrophys.* **341** L1 (1999)
15. Efremov Yu N *Pis'ma Astron. Zh.* **25** 100 (1999) [*Astron. Lett.* **25** 74 (1999)]
16. Larsen S S, Richtler T *Astron. Astrophys.* **345** 59 (1999)
17. Elmegreen B G, Efremov Yu N, Larsen S S *Astrophys. J.* **535** 748 (2000)
18. Paczynski B, astro-ph/9909048; to be publ. in *The Largest Explosions Since the Big Bang*: *Supernovae and Gamma Ray Bursts* (Eds M Livio, K Sahu, N Panagia) (Cambridge: Cambridge Univ. Press, 1999)
19. Postnov K A, Prokhorov M E, Lipunov V M, astro-ph/9908136
20. Cole A A et al. *Astron. J.* **114** 1945 (1997)
21. Davis M B, in *IAU Symp.* 174 (Eds P Hut, J Makino) (Dordrecht: Kluwer, 1995) p. 243
22. Fryer C, Kalogera V *Astrophys J.* **489** 244 (1997)
23. Portegies Zwart S, McMillan S L W *Astrophys. J.* **528** L17 (2000)
24. Milgrom M, Usov V V, astro-ph/0001283 (submitted to *Astrophys. J. Lett.)*
25. Efremov Yu N, Ehlerova S, Palous J *Astron. Astrophys.* **350** 457 (1999)
26. Usov V V *Nature* (London) **357** 344 (1992)
27. Usov V V, astro-ph/9909435
28. Ahn S-H *Astrophys. J.* **530** L9 (1999)
29. Kroupa P, astro-ph/0001202
30. Chevalier R A, Li Z-Y *Astrophys. J.* **520** L29 (1999)
31. Rodriguez L F, Mirabel I F, astro-ph/9811250
32. Dubner G M et al. *Astron. J.* **116** 1842 (1998)
33. Fargion D *Astron. Astrophys. Suppl.* **138** 507 (1999)
34. Efremov Yu N, Fargion D, astro-ph/9912562

Persistent currents and magnetic flux trapping in a multiply connected carbon nanotube structure

V I Tsebro, O E Omel'yanovskiĭ

1. Carbon — this wonderful element that forms the basis for a multitude of natural and synthetic materials — amazed the world once again in the last years of the past century. In addition to its well-known solid crystallographic forms like diamond and graphite, it appeared before the world in the form of fullerenes and nanotubes. Ten years have not yet elapsed since the first report [1] of the discovery of multilayer carbon nanotubes in the cathode deposit of electric arc synthesis of fullerenes. It comes as no surprise that their properties have been the object of much concentrated attention and the subject of intensive research (see, e.g., reviews [2–6]). Among recent papers concerned with the electronic properties of carbon nanotubes, we would like to point out the experimental and theoretical papers on coherent electron transport in single-layer nanotubes [7–11] and the theoretical papers [12–14] that consider the related issue of persistent circulation currents in closed toroidal nanotubes. In particular, the data obtained by the method of transport spectroscopy [7, 8] suggest that coherent electron transport occurs in single-layer nanotubes at low temperatures. This transport occurs over very long distances — according to the estimates made by Tans et al. [7], up to the full length of a nanotube several micrometers long.

The subject of our report is the experimental discovery [15] of the effect of magnetic flux trapping in a multiply connected structure of multilayer carbon nanotubes that is formed in cathode deposits during the electric arc process for their synthesis. This flux trapping occurs just as it does in a multiply connected filamentary superconductor similar to the so-called 'Mendelssohn sponge' [16] — a multiply connected system of thin superconducting filaments in a normal matrix. Therefore, it sounds as if it were a statement of the superconductivity of this structure, this being so for a very high temperature (as will be seen from the following, at temperatures well above room temperature). However, superconductivity in the usual sense of the word (the formation of a Bose condensate of Cooper pairs below the transition point) is not the only explanation of the effect discovered. It is possible that we are dealing with the first experimental observation of so-called persistent currents which circulate through the closed mesoscopic paths of a multiply connected structure of this type. The problem of persistent currents and of the construction of the ground state that allows for their existence in mesoscopic closed objects [17] and also results in the trapping of magnetic flux was considered theoretically in several recent papers [18–20] (also see Refs [12–14]). One way or the other, the case in point is not some weak (hardly detectable) or controversial (as regards interpretation) phenomenon, but a quite noticeable macroscopic effect. It is as if we were really dealing with a conventional filamentary superconductor or, say, a type II superconductor with an ultimately weak first critical field.

2. Briefly what led us to discover the effect. It is well known (see, e.g., Ref. [21]) that the anomalous high value of

the diamagnetic susceptibility of graphite for a magnetic field orientation perpendicular to the graphite planes is associated with a very large value of the effective circulation radius ρ of ring inductive currents in the Larmor – Langevin formula $\chi = -(Ne^2/4mc^2)\rho^2$, where c is the velocity of light, m and e are the electron mass and charge, and N is Avogadro's number (for molar susceptibility). For the π electrons in graphite, this radius is 7.8 Å, i.e., the circulation loop area encompasses approximately 36 unit cells of graphite. This leads to a magnitude of $\chi \sim 10^{-4}$ emu mol^{-1}, which is approximately 25 times the diamagnetic susceptibility of the aromatic π electrons of benzene and approximately two orders of magnitude higher than that for the aromatic π electrons of benzene or, say, the diamagnetic susceptibility of diamond.

With the advent of carbon nanotubes, the question naturally arose whether a giant diamagnetism is possible in an ordered system of nanotubes (whose axes are aligned with the magnetic field) if the ring currents in response to the applied magnetic field circulate over the walls of the nanotubes around their axes. In this case, for an average nanotube radius of ~ 80 Å, the diamagnetic susceptibility of this system should be 100 times that of graphite. The strong anisotropy of the diamagnetic susceptibility of an artificially ordered thin-layer system of carbon nanotubes discovered in Ref. [22] seemingly counts in favor of this suggestion, which is certainly simple and qualitative in character. However, the possible giant diamagnetism of carbon nanotubes whose axes are aligned with the magnetic field is coming to be the subject of a more rigorous treatment, too. Here, it is pertinent to note the paper by Ovchinnikov [23], who carried out calculations of the diamagnetic susceptibility of carbon nanotubes in the context of a simple model employing the Hückel Hamiltonian (the Hückel model). It was shown that the diamagnetic susceptibility of the nanotubes aligned with the magnetic field can be as high as $\sim 10^{-2}$ emu mol^{-1}, which is two orders of magnitude higher than that in graphite for a magnetic field oriented perpendicular to the graphite planes.

In an attempt to experimentally verify the conclusions of Ref. [23], we undertook studies of the magnetic properties of cathode deposit samples. The point is that samples containing highly ordered nanotubes in reasonable quantity are extremely hard to prepare artificially.[1] This impelled us to turn to the samples of carbon deposits produced at the cathode during the electric arc synthesis of multilayer nanotubes in the context of their production technology which has now become traditional [2, 3, 5, 25]. The point is that it was believed, until a certain point in time (and this was suggested, e.g., by the data of Ref. [25]), that the carbon columns of the columnar structure of the central deposit region referred to in the subsequent discussion contain multilayer nanotubes aligned with the column axes and that it is therefore possible to obtain a macroscopic object with a given nanotube orientation for magnetic measurements by collecting the sample of oriented columns or simply using the preferred central deposit region as the sample.

More recently, it turned out that this is not the case. Dedicated electron microscope research of the inner structure of cathodic deposits was performed by N A Kiselev et al. in the Shubnikov Institute of Crystallography, Russian Academy of Sciences, and by A B Ormont in the Institute of Radio Engineering and Electronics, Russian Academy of Sciences [26]. It revealed that the nanotubes in different deposit regions, including carbon columns, are oriented rather chaotically and primarily at blunt angles to its growth axis and the axis of the columns, and therefore we may not speak of the preparation of samples with a given nanotube orientation. The structural studies conducted [26] made it possible to reasonably amply determine the structure of the central region of the cathode deposit and the pattern of nanotube distribution within it (Fig. 1). This allowed us to relate this pattern to the effect of magnetic flux trapping and its anisotropy discovered in the measurements of magnetic properties.

3. The samples investigated in our work were prepared by A P Moravskiĭ in the Institute of Chemical Physics, Russian Academy of Sciences. They were small fragments extracted from the central region of the carbon deposits produced on the cathode in the synthesis of multilayer nanotubes by the electric discharge technique. This technique [1 – 3, 5, 25], which also underlies the most efficient and therefore widely accepted technology of preparing fullerenes [27, 28], involves thermal vaporization of the graphite electrode (the anode) in the arc discharge plasma in a helium atmosphere.[2] Intensive thermal sputtering of the anode material results, causing its transfer to the cooler cathode. There, a cathodic deposit builds up, which contains carbon nanotubes in some quantity or another, depending on the discharge mode. In the processing sequence for obtaining a pure nanotube material, such cathodic deposits are regarded as an intermediate product, which is subjected to special intensive processing (ultrasonic dispersion in an organic solvent, centrifugal processing, strong oxidizing agents) to obtain a material made up almost entirely of multilayer nanotubes freed from nanoparticles and other carbon associations. Clearly, the internal structure of the cathode deposit, initially fixed during condensation of the carbon material on the cathode, is completely destroyed in this case. According to Kisilev et al. [26], the initial structure contains variously interconnected multilayer nanotubes in the form of a multiply connected mesh of the outer shells of carbon columns or a nanotube web in the space between them. This is the reason why in our experiments recourse was intentionally made to the fragments of cathode deposits not subjected, upon completion of the arc discharge, to any special treatment destroying the material structure.

As already noted, the qualitative composition and the internal structure of the deposits prepared in different technological modes, including those which we used to prepare the samples for magnetic measurements, were studied comprehensively in Ref. [26]. The findings of this work are of prime importance in the interpretation of the data on magnetic properties obtained in our work, because they made it possible to reconstruct in sufficient detail the internal structure of the cathode deposits and reveal the existence of a

---

[1] In the above-cited paper by Chauvet et al. [22] devoted to the study of ordered nanotubes, advantage was taken of a special multistage procedure [24]: a nanotube suspension dispersed in ethanol was made to flow through a special ceramic filter with pores ~ 0.2 μm in diameter, after which the nanotube sediment on the opposite side of the filter was transferred onto a polymer (teflon) film substrate merely by pressing the filter against the polymer. According to Refs [22, 24], the nanotubes in the resultant layers were oriented primarily perpendicular to the substrate surface.

[2] In our case, 200-mm-long graphite rods 6 mm in diameter were used as the anode. The discharge current was 65 A. The helium pressure in the chamber ranged from 200 to 500 Torr in different series of deposit preparation.
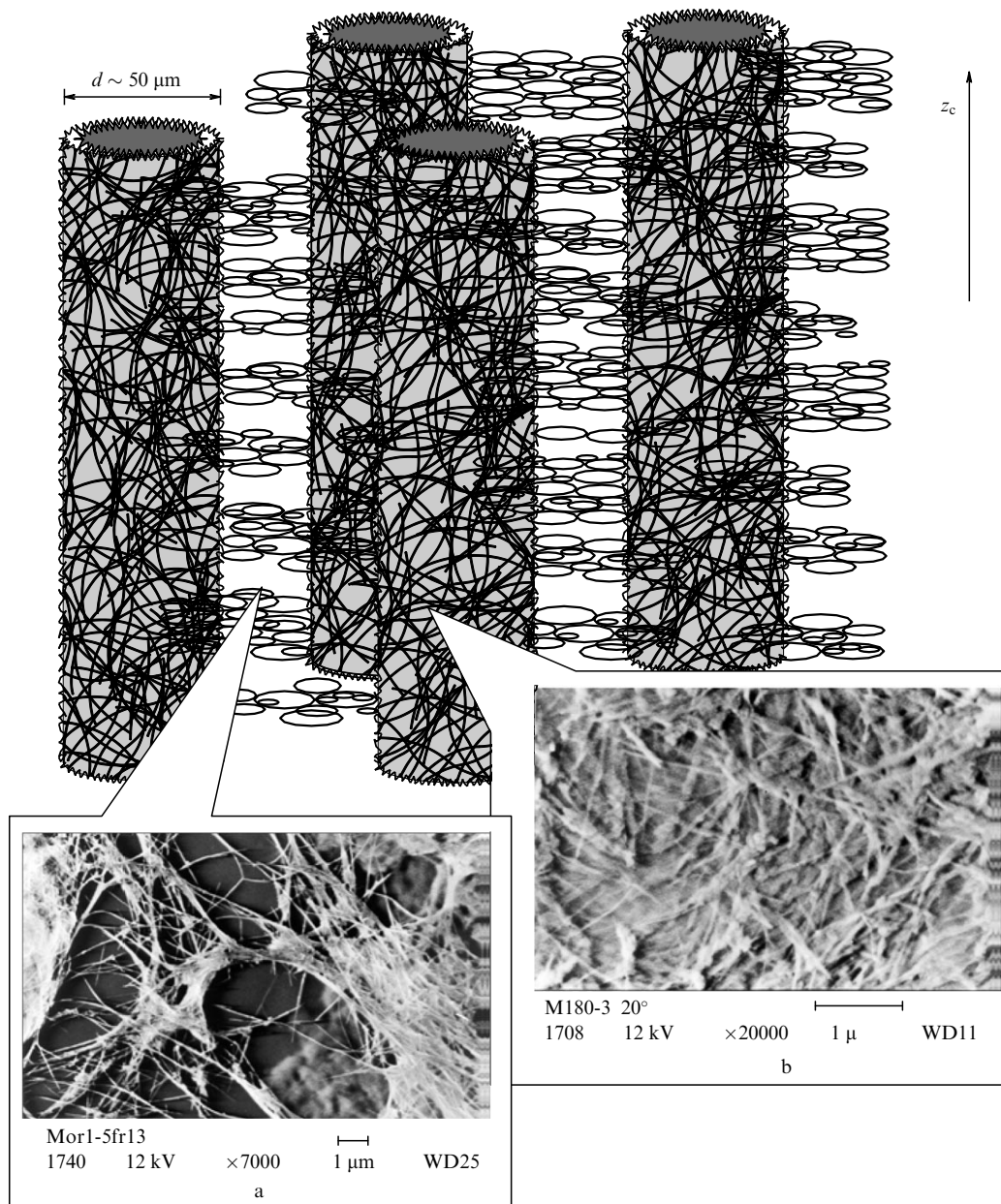
Figure 1. Model of the columnar structure of the cathode deposit samples studied. The column axes z_c are aligned with the axis of deposit growth. Multilayer nanotubes appear in the form of a dense multilayer network on the side column surfaces and in the form of a sparse nanotube web in the space between them. The electron microscope images of the multilayer nanotubes on the side column surfaces (b) and in the space between them (a) were borrowed from Ref. [26].

multiply connected nanotube structure in it. According to Ref. [26], the central region of the cathode deposit has a columnar structure aligned with the axis of deposit growth, and this is consistent with the data of other authors (see, e.g., Ref. [25]). In the samples studied in our work, the carbon columns of such a columnar structure are, according to Ref. [26], made up of three main components: multilayer nanotubes 5 to 45 nm in diameter (the most probable value is ~ 15 nm), multilayer polyhedral particles measuring 20-to-90 nm, and curved graphitized structures. Their relative abundances and characteristic dimensions are determined by the parameters of the arc process (for more detail, see Ref. [26]). While all the three components are found inside the columns, the outer column shell consists primarily of interwoven multilayer nanotubes, only. It is also significant

that multilayer nanotubes in the form of a peculiar nanotube web are present in substantial amounts in the space between the columns, too. As for the nanotube orientation, the nanotubes from different deposit regions (in the carbon columns and in the space between them) are, as already noted, oriented primarily at angles above 45° to the axis of deposit growth.

Figure 1 is a conventional (for visual clarity) representation of the columnar-structure model of the cathode deposits studied in our work. The carbon columns (the average column diameter is ~ 50 μm) are shown spaced at some distance (in reality [26], the column separation ranges from 10 to 15 μm). The nanotubes in the form of a dense multilayered interwoven mesh are located on the side surfaces of the columns. The space between the columns is

occupied by a relatively sparse multiply connected nanotube web. The examples of electron microscope images of the multilayer nanotubes on the side column surfaces and in the space between them, which are given in Fig. 1, were borrowed from Ref. [26].

4. The samples for the measurements of magnetization curves were either (i) carbon columns extracted from the central deposit region, assembled and secured together by a negligible amount of nonmagnetic glue, and aligned with a common z_c axis or (ii) small volume cylinders ~ 2.5 mm in diameter and up to 5 mm in length cut out from the central deposit region along the growth axis z_d. In the former case, the sample masses were $1-5$ mg, and their magnetic properties were measured in weak (< 500 Oe) magnetic fields employing a SQUID magnetometer having a magnetic moment sensitivity on the order of 5×10^{-9} emu. An optical image of the end profile of one of these samples with a mass of 1.6 mg is shown in Fig. 2.
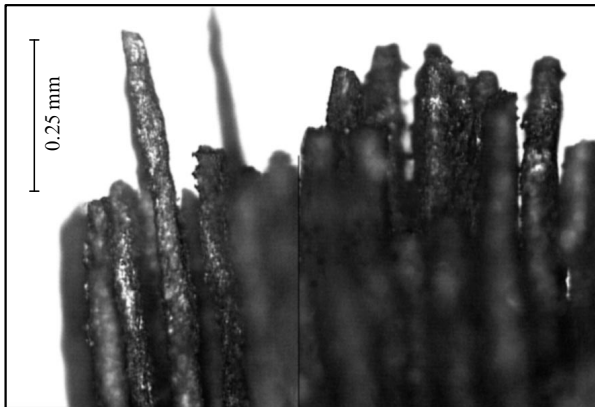

Figure 2. Optical image of the end profile of one of the samples made up of carbon columns assembled together.

In the latter case, the weight of the cylindrical samples cut out was on the order of several tens of milligrams. They were intended for magnetic measurements in strong magnetic fields employing an autocompensation magnetometer with a capacitance sensor [29].

5. *Magnetic flux trapping in weak magnetic fields.* As an example, Fig. 3 gives the results of magnetization measurements with a SQUID magnetometer for $T = 4.2$ K. The sample was assembled from carbon columns (see Fig. 2) and the magnetic field was directed perpendicular to the column axis z_c, i.e., along the normal to their cylindrical surface. One can see that a virtually linear $M(H)$ dependence (curve *1*) occurs upon the initial increasing of the field,[3] with the slope (magnetic susceptibility χ) equal to $\chi = -3.8 \times 10^{-4}$ emu mol^{-1} for the given sample. On decreasing the magnetic field (curve *2*), the trapped magnetic flux persists in the sample; in this particular case, this flux corresponds to a paramagnetic moment $M_r \approx 0.04$ emu mol^{-1}. On subsequent cycling of the magnetic field from -500 to 500 Oe (curves *2* and *3*), a characteristic hysteresis loop is observed.

---

[3] Provided the sample had been kept at room temperature for a long time (for more than three days) to ensure a nearly complete relaxation of the magnetic flux trapped in the preceding experiments (see below).
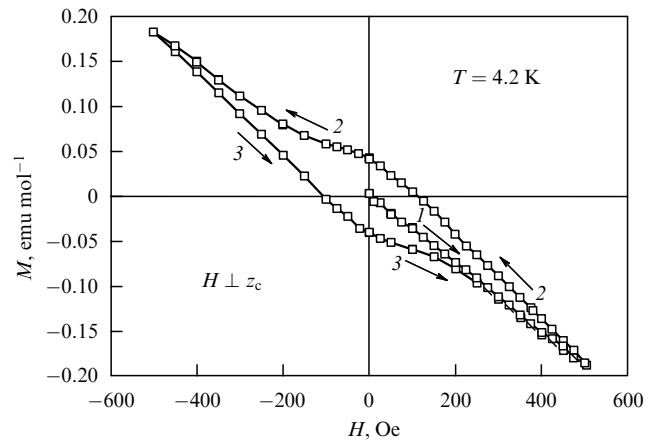

Figure 3. Hysteresis loop of the magnetization curve for one of the samples made up of carbon columns assembled together; $T = 4.2$ K, the sample mass is 1.6 mg. The magnetic field is directed perpendicularly to the axis of the carbon columns.

The time and temperature dependences of the magnitude of the trapped magnetic moment M_r were measured. Long (up to 20 h) observations of M_r at liquid-helium temperature do not reveal any noticeable attenuation of this quantity to within the experimental error (~ 1 %). This allows a statement that the currents induced in the sample are persistent at a low (liquid-helium) temperature. A noticeable relaxation of the trapped magnetic moment by the exponential law with characteristic relaxation times $\tau_0 \sim 150$ h is revealed even on heating the samples to an intermediate temperature level (~ 20 K). Measurements of the $M_r(t)$ time dependences at room temperature showed that the relaxation times τ_0 remain rather long, on the order of 15 h, even at so high a temperature. To practically restore the initial state of the samples (say, to reduce the magnitude of M_r to less than 1% of the initial level), the samples have to be kept at room temperature for about three days. Therefore, the temperature governs the relaxation time τ_0 rather than the magnitude of the trapped magnetic moment M_r. Figure 4 shows the typical
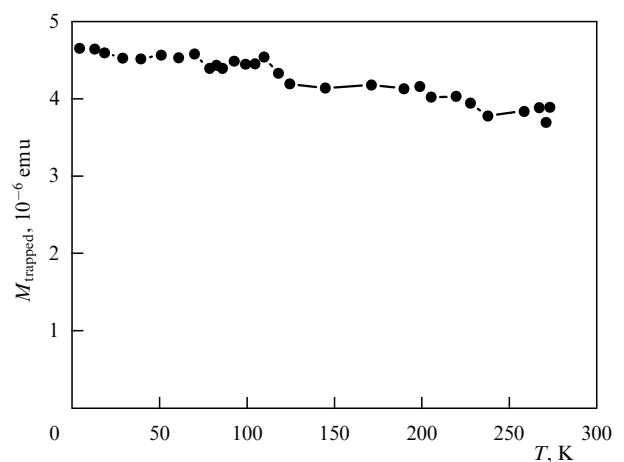

Figure 4. Temperature dependence of the magnitude of the trapped moment in the course of a three-hour sample warming from the liquid-helium temperature to room temperature. For a rapid warming to room temperature with subsequent cooling to the liquid-helium temperature, the magnitude of the trapped moment remains invariable.

temperature dependence of the magnitude of the trapped magnetic moment M_r for a slow (three-hour) warming of the sample from the liquid-helium temperature to room temperature inside the measuring part of the magnetometer. In the case of a rapid warming to room temperature, the magnitude of the trapped moment remains constant. This implies that at room temperature, too, the currents induced in the sample are persistent and the relaxation of the trapped flux is most likely determined by the activation mechanism, as is the case in type II superconductors over a broad temperature range below the superconducting transition temperature (see, e.g., Refs [30, 31]).

Repeated examination of different samples prepared both from different parts of the same deposit and from different deposits showed that the hysteresis of magnetization curves took place nearly in all the cases — only its magnitude changes, varying from sample to sample over a very wide range. For some samples, the contribution of the irreversible part of magnetization was very small, and the hysteretic properties of the $M(H)$ curves could be satisfactorily illustrated only by giving the difference dependences of the form $M(H) - \chi_0 H$ (where χ_0 is the static magnetic susceptibility at the extreme points of the hysteresis loop). In this sense, Fig. 3 presents our best results as regards the magnitude of the effect obtained in a weak magnetic field with samples of carbon columns.

Assuming that the magnetic flux trapping takes place primarily in the cells of the multilayer interwoven mesh of nanotubes on the surface of carbon columns, one would expect a strong anisotropy of the effect of magnetic flux trapping, because the cells of this mesh are mostly oriented normally to the side surface of the columns. Indeed, the magnitude of the hysteresis of magnetization curves depends strongly on the direction of the magnetic field relative to the axis of the columns z_c, the effect being maximum when $H \perp z_c$. As an example, we refer to Fig. 5, which gives, for one of the samples studied, the entire hysteresis loop of the type $M(H) - \chi_0 H$ for $H \perp z_c$ and the initial curves $M(H) - \chi_0 H$ on increasing and decreasing of the magnetic field with an orientation $H \parallel z_c$. One can see that the magnitude of the trapped magnetic flux M_r for $H \parallel z_c$ is approximately four times smaller than for $H \perp z_c$.

6. Irreversibility of magnetization curves in strong magnetic fields. The measurements in strong magnetic fields were conducted only for $T = 4.2$ K in the nonuniform field of a superconducting solenoid using an autocompensation magnetometer with a capacitance sensor [29]. The measurements were carried out on cylindrical samples cut out from the central deposit region along its growth axis z_d. In these experiments, we had no way of changing the magnetic field direction in the superconducting solenoid (of niobium – tin tape), and therefore the $M(H)$ curves were measured on increasing and decreasing of the field in one direction. To illustrate, Fig. 6 shows the magnetization curves for one of the samples on increasing and decreasing of the field for two orientations: $H \parallel z_d$ (curves 1) and $H \perp z_d$ (curves 2). These data illustrate the general pattern obtained in strong magnetic fields. First, the magnetization curves are essentially nonlinear, which is testimony to the intricacy of magnetic interactions in the multiply connected nanotube system (it is conceivable that a change of the orientation of the current loops occurs under the influence of the magnetic field). In this case, a strong nonlinear field dependence of the magnetization anisotropy exists, when a sharp increase in the $M_\parallel / M_\perp$ ratio in the $0 - 20$ kOe field intensity range is replaced by slow monotonic growth up to values $M_\parallel / M_\perp \sim 1.5$ for $H \sim 100$ kOe. Second, the magnetization curves are irreversible in the range of strong magnetic fields, too. In this case, as with weak magnetic fields and samples of carbon columns, there occurs a noticeable anisotropy of the magnitude of the hysteresis of the $M(H)$ curves. However, the magnitude of hysteresis is significantly larger when the field H is parallel to the axis of deposit growth z_d and, hence, to the axes of carbon columns. In this case, a significant contribution to the magnitude of the trapped flux is presumably made by the multiply connected nanotube structure (nanotube web) in the space between the columns, whose cells are oriented normally to the axis of deposit growth (see Fig. 1). We also note that in this case it was possible, for some samples, to attain a value of the residual moment $M_r \sim 2$ emu mol^{-1} on complete field removal from the strong-field range for $H \parallel z_d$. It might be well to point out that the quantumwise trapping of magnetic
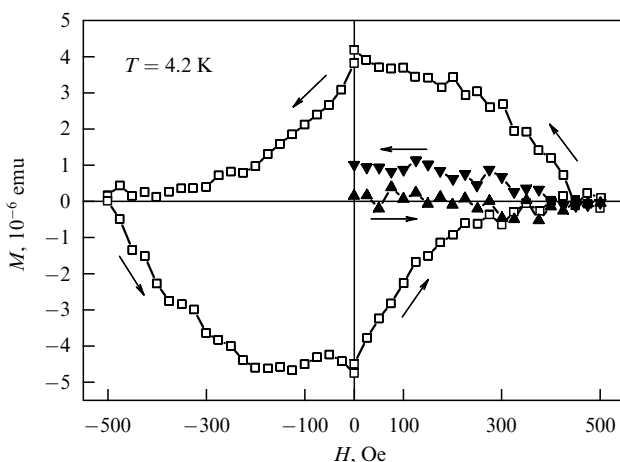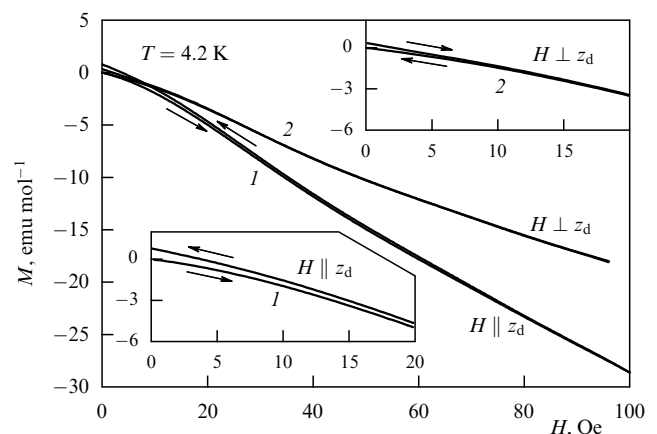
Figure 5. Anisotropy of the hysteresis loop of magnetization curves for $T = 4.2$ K. Plotted are the absolute values of the magnetic moment minus $\chi_0 H$ (see the text): ($\square$) the entire hysteresis loop for $H \perp z_c$; the initial increasing ($\blacktriangle$) and decreasing ($\blacktriangledown$) of the magnetic field for $H \parallel z_c$.

Figure 6. Strong-field magnetization curves of a cylindrical volume sample cut out from the central deposit region along the growth axis z_d. The $M(H)$ curves on increasing and decreasing of the field are shown for the magnetic field orientation parallel (1) and perpendicular (2) to the axis of deposit growth; $T = 4.2$ K, the sample mass is 67 mg. The insets show the initial portions of the curves for different orientations of the magnetic field relative to z_d.

flux supposedly occurs, in the case of strong magnetic fields, in smaller cells of the multiply connected nanotube structure, which explains the higher values of the residual moment M_r.

7. Therefore, a study was made of sample fragments of the cathode carbon deposits, not destroyed during special processing to extract and clean the multilayer nanotubes contained in the deposits. We found that they can carry magnetic field-induced currents, which persist at low (liquid-helium) temperatures or decay very slowly at high (room) temperatures. This property is exhibited by magnetization curves, whose irreversible character is clearly defined, i.e., magnetic flux trapping occurs in the samples, as in a multiply connected superconducting structure.

The reason why the trapped moment relaxes at high temperatures remains to be solved. If it is assumed that we are dealing with real superconductivity of a multiply connected nanotube system, this relaxation should be ascribed to the activation mechanism, as in type II superconductors, when a flux quantum-carrying vortex filament overcomes, owing to the thermal motion, the pinning force that confines it to a given pinning center [30, 31]. In our case, this pinning center is a nanotube mesh cell that has trapped one or several quanta of the magnetic flux. In this connection, we note that the frequently observed scatter of experimental points in the hysteretic loops of magnetization curves (see Fig. 5) appears to be nothing but a manifestation of the flux jumps known for type II semiconductors, because the accuracy of low-temperature measurements with a SQUID magnetometer is two orders of magnitude higher than the observed scatter of experimental points.

If the multiply connected nanotube system is actually superconducting, clearly a very high value of the super-conducting transition temperature T_c should be expected for this system. We conducted a dedicated experiment wherein a sample, which was assembled of carbon columns, with a magnetic moment trapped at low temperatures was held at a temperature of $100\,^\circ$C for two hours. In this case, the magnitude of the trapped moment reduced only twofold after this exposure. This implies that T_c of the system should be significantly higher than 373 K (!).

As already noted, it is not improbable that we are dealing not with superconductivity, but with the first experimental observation of persistent currents induced by a magnetic field which circulate along closed mesoscopic paths (mesh cells) of the multiply connected nanotube structure. In this case, the slow relaxation of persistent currents at high temperatures may be related to the existence of parallel current channels with an inelastic scattering of current carriers, and the interaction between the ideal channels with a ballistic mode of carrier motion and the scattering channels is responsible for the relaxation observed. We have already mentioned a series of theoretical papers [12–14, 18–20] concerned with different possibilities for the existence of persistent currents for several mesoscopic objects, including closed toroidal single-layer carbon nanotubes [13, 14]. Furthermore, one of these more general papers [20] points out directly that among the mesoscopic objects that may harbor such currents are carbon nanotubes.

The fact that coherent electron transport takes place in single-layer carbon nanotubes at low temperatures follows from the results of experimental papers [7, 8, 11]. The superconductivity of single-layer carbon nanotubes induced by the neighborhood effect (the nanotube was placed between two superconducting metallic contacts) at a temperature

below 1 K was observed by Kasumov et al. [32]. However, in connection with the subject of the present communication, the findings of Frank et al. [33] are extremely important to us. They showed the measured room-temperature conductivity of multilayer carbon nanotubes with diameters from 5 to 25 nm and up to 10 μm in length to be quantum in the sense that it does not depend on the nanotube length and its diameter, the conductivity being equal to $G_0 = 2e^2/h = (12.9\ \text{k}\Omega)^{-1}$. What is quite significant, multilayer carbon nanotubes at room temperature are, according to Frank et al. [33], capable of carrying a current with a density of over 10^7 A cm^{-2}. The conductivity of multilayer nanotubes was measured in Ref. [33] with a scanning tunneling microscope, a single nanotube playing the part of a needle whose second end was sunk in a liquid metal to ensure electrical contact. For a density of electric current through the nanotube of $\sim 10^7$ A cm^{-2}, the power dissipated by the nanotube (owing to a finite quantum resistance) was ~ 3 mW. This implies, as noted by the authors, that if all this power were scattered uniformly over the entire length of the nanotube (~ 1 μm in length and ~ 20 nm in diameter), its temperature would be as high as 20000 K. All this suggests that the high-temperature electric transport in multilayer carbon nanotubes is ballistic and proceeds without heat release.

Hopefully, future research will elucidate the true nature of magnetic flux trapping and persistent currents in the multiply connected carbon nanotube structure of cathode deposits. We only remark that all the papers cited in our communication testify to the fact that carbon nanotubes recently revealed to the world are objects with extremely interesting properties, one of the nontrivial properties being dissipation-free electron transport. Carbon nanotube research is still in its infancy.

Note. It is a cause for regret that the multiply connected nanotube structure in the series of cathode deposit samples studied in our work was devoid of long-term stability and would collapse on long storage of the samples in the open air. This fact was not reflected in Ref. [15] because the check experiments were performed somewhat later. These experiments showed that the magnitude of the trapped magnetic moment decreases severalfold after exposing the samples to air for one year and becomes hardly observable after 3-4-years storage. It seems likely that a deoxidation of the nanotube–nanotube junctions occurs with the breaking of weak bonds and eventually the multiple connectedness of the system as a whole. This assumption invites special investigation. But the very fact of such aging indicates that special steps should be taken to preserve the multiply connected nanotube structure over a long period of time.

References

1. Iijima S *Nature* (London) **354** 56 (1991)
2. Ebbesen T W *Phys. Today* **49** (6) 26 (1996)
3. Smalley R E *Rev. Mod. Phys.* **69** 723 (1997)
4. Lozovik Yu E, Popov A M *Usp. Fiz. Nauk* **167** 751 (1997) [*Phys. Usp.* **40** 717 (1997)]

5. Eletskiĭ A V *Usp. Fiz. Nauk* **167** 945 (1997) [*Phys. Usp.* **40** 899 (1997)]
6. Dresselhaus M S, Dresselhaus G, Eklund P C *Science of Fullerenes and Carbon Nanotubes* (San Diego: Acad. Press, 1996)
7. Tans S J et al. *Nature* (London) **386** 474 (1997)
8. Bockrath M et al. *Science* **275** 1992 (1997)
9. White C T, Todorov T N *Nature* (London) **393** 240 (1998)
10. Egger R, Gogolin A O, cond-mat/9803128; *Eur. Phys. J. B* **3** 281 (1998)
11. Bockrath M et al. *Nature* (London) **397** 598 (1999)
12. Haddon R C *Nature* (London) **388** 31 (1997)
13. Lin M F, Chuu D S *Phys. Rev. B* **57** 6731 (1998)
14. Odintsov A A, Smit W, Yoshioka H, cond-mat/9805164
15. Tsebro V I, Omel'yanovskiĭ O E, Moravskiĭ A P *Pis'ma Zh. Eksp. Teor. Fiz.* **70** 457 (1999) [*JETP Lett.* **70** 462 (1999)]
16. Mendelssohn K *Proc. R. Soc. London Ser. A* **152** 34 (1935)
17. Büttiker M, Imry Y, Landauer R *Phys. Lett. A* **96** 365 (1969)
18. Szopa M, Zipper E *Int. J. Mod. Phys. B* **9** 161 (1995)
19. Stebelski M, Lisovski M, Zipper E *Eur. Phys. J. B* **1** 215 (1998)
20. Lisovski M, Zipper E, Stebelski M *Phys. Rev. B* **59** 8305 (1998)
21. Haddon R C *Nature* (London) **378** 249 (1995)
22. Chauvet O et al. *Phys. Rev. B* **52** 6963 (1995)
23. Ovchinnikov A A *Phys. Lett. A* **155** 95 (1994)
24. De Heer W A et al. *Science* **268** 845 (1995)
25. Colbert D T et al. *Science* **266** 1215 (1994)
26. Kiselev N A et al. *Carbon* **37** 1093 (1999)
27. Eletskiĭ A V, Smirnov B M *Usp. Fiz. Nauk* **163** 33 (1993) [*Phys. Usp.* **36** 202 (1993)]
28. Eletskiĭ A V, Smirnov B M *Usp. Fiz. Nauk* **165** 977 (1995) [*Phys. Usp.* **38** 935 (1995)]
29. *Null-balance Magnetometer with Capacitance Sensor. Internal Specification.* International Laboratory of High Magnetic Fields and Low Temperatures (Wroclaw, 1998)
30. Campbell A M, Evetts J E *Critical Currents in Superconductors* (London: Taylor and Francis, 1972)
31. Brandt E H *Rep. Prog. Phys.* **58** 1465 (1995)
32. Kasumov A Yu et al. *Science* **284** 1508 (1999)
33. Frank S et al. *Science* **280** 1744 (1998)

Two-dimensional excitonic polaritons and their interaction

V D Kulakovskiĭ, A I Tartakovskiĭ,
D N Krizhanovskiĭ, A Armitage,
J S Roberts, M S Skolnick

Considerable recent attention has been focused on semiconductor microcavities (MCs) with plane Bragg mirrors owing to the possibility of profoundly altering the exciton properties in quantum wells placed in the antinode of the electromagnetic field [1]. The system of strongly interacting excitons and photons in an MC is described in terms of excitonic MC polaritons. These polaritons are realized only in an MC with a relatively high Q factor, when the interaction between the photon mode (C) in the MC and the exciton mode (X) in the quantum well exceeds their broadenings. The excitonic polaritons in plane MCs are quasi-two-dimensional and are characterized by extremely small masses, $\sim 10^{-5} m_0$, and large dimensions, on the order of a micron [2]. Unlike volume excitonic polaritons, which are stable quasiparticles, they have a very short lifetime, on the order of several picoseconds. The qualitative difference derives from the fact that MC polaritons annihilate without conservation of the momentum in the direction perpendicular to the plane of the quantum well.

The quasi-two-dimensional polaritons in MCs constitute a very interesting object of research. First, the light confinement in an MC is responsible for a strong multiplication of the electromagnetic field and should therefore result in a dramatic enhancement of nonlinear effects. Second, the MC polaritons are bosons. Owing to the smallness of their mass, a polariton system admits, unlike an exciton one, attainment of a significant filling of states for a relatively low overall density, whereby the effect of the internal fermion structure of the excitons can be neglected. In this case, the features predicted for bosons, like stimulated scattering and condensation in the momentum **k** space (Bose condensation) [3], would be expected to manifest themselves in the system of MC polaritons.

Among the manifestations of stimulated scattering is a superlinear increase of the polariton radiation at high excitation densities. This mode was discovered by Pau et al. [4] in studies of a GaAs/AlAs MC under intense light excitation with photon energies $\hbar\omega$ exceeding the width of the GaAs forbidden band E_g. The effect was interpreted as a sequel to the Bose condensation of polaritons and was termed 'boser.' More comprehensive studies [5] revealed that the stimulated emission arises in circumstances where the Coulomb interaction in the system is strongly screened owing to a high density of photoexcited carriers and the exciton – photon interaction is suppressed, i.e., is realized in the mode of weak interaction. Relying on their calculations, Kira et al. [5] arrived at the conclusion that there is no way of realizing a boser in MC structures in the mode of strong interaction. However, the observation of the superlinear polariton luminescence mode in the strong interaction mode was reported recently in II – VI semiconductor compound MC structures, where the exciton binding energy and, hence, the critical density is significantly higher than in GaAs [6]. However, it is pertinent to note that the excitation with $\hbar\omega > E_g$ is extremely inefficient for the realization of a high filling of the polariton states, because the time for the relaxation to the polariton states at the bottom of the lower polariton branch (LPB) is comparable with the polariton lifetime.

Here, in order to realize a high LPB filling, we resorted to the resonance excitation either to the bottom of the upper polariton branch (UPB) or directly to the LPB $1 - 3$ meV above its minimum. Furthermore, unlike earlier papers, we excited the system using circularly polarized light. It turned out that the polariton spin relaxation time τ_s in this case was significantly shorter than their lifetime τ_l. We were therefore able to realize a spin-polarized polariton system with a relatively high degree of spin polarization and observe a variety of nonlinear effects both in the radiation intensity and in the degree of circular polarization.

We studied nonlinear effects in the emission of a GaAs/AlAs MC with a set of InGaAs quantum wells in the active layer under resonance of the photon and exciton modes at $k = 0$, when the polaritons with $k = 0$ are half exciton and half photon in nature. A tunable titanium – sapphire laser was used to excite the MC luminescence. The sample was placed in a cryostat at a temperature of $1.8 - 10$ K. The experiments were carried out on structures with a Rabi splitting of $5 - 7$ meV and an energy mismatch of the X and C modes $|\varDelta| < 0.6$ meV. The polariton dispersion law measured for low excitation densities is shown in Fig. 1b.

Figure 1a gives the MC emission spectra recorded under nonresonance excitation above E_g. For low P, the emission